Quantized thermal conductance via phononic heat transport in nanoscale devices at low temperatures

M. Käso* and U. Wulf†

Department of Theoretical Physics, Brandenburg University of Technology Cottbus, Konrad-Wachsmann-Allee 1, 03046 Cottbus, Germany

(Received 6 May 2013; revised manuscript received 19 September 2013; published 28 April 2014)

We study phononic heat transport in nanoscale devices. In the nonequilibrium Green's function formalism, an analytical small-frequency expansion of the phonon current transmission is derived for an arbitrary oscillator chain with typical contact-device-contact structure. Applying this expansion in a Landauer formula, it is possible to construct a systematic low-temperature expansion of the thermal conductance. It follows that quantized thermal conductance occurs as a plateau of the thermal conductance divided by the temperature within second order of the temperature expansion for completely heterogeneous systems as long as the product of force constant and oscillator mass is identical in both contacts, independent of the scattering area. Beyond this plateau, the higher-order terms of the low-temperature expansion yield a finite-temperature correction exhibiting the form of a cubic power law depending on the details of the scattering area. These findings are in agreement with experiments and numerical calculations. Our general results are applied to a double junction chain, where we find as the first phenomenon beyond our low-temperature expansion a second plateau. This plateau is associated with a thermal phase averaging of the phonon transmission, which leads for increasing temperatures to an independence of the thermal conductance from the device length.

DOI: 10.1103/PhysRevB.89.134309 PACS number(s): 63.22.−m, 44.05.+e

I. INTRODUCTION

In the past years, the problem of mesoscopic heat transport in nanoscale devices such as thermal rectifiers and diodes [1], thermal transistors [2], thermal logical gates [3], and thermal memory [4] has attracted an increasing amount of attention. As the device dimensions shrink to the magnitude of typical phonon wavelengths, scattering in the devices is reduced and the wave nature of phonons becomes more and more important. In the arising quantum transport problems, heterogeneities in the device structure and associated interface scattering effects play a central role.

The study of heat transport in one-dimensional systems with a typical contact-device-contact structure has led to the concept of the quantization of the thermal conductance $\Lambda(T)$ in multiples of $\pi^2 k_B^2 T/3h$, universal for fermions [5,6], bosons [7–10], and anyons [11–13]. Here, we focus on the phononic thermal conductance where quantization has been observed experimentally [14]. There exist three essential conditions for the occurrence of this effect [7,14]. First, optical phonons have to be negligible, second, the upper cutoff frequency of the acoustic phonons has to be negligible as well, and, third, perfect transmission should exist for all relevant acoustic phonon modes. It is found that the first two conditions can be met in any thermal junction at low enough temperatures. The first condition becomes fulfilled because optical phonons exhibit a lower cutoff frequency so that their occupation freezes out. The second condition becomes fulfilled because the correction to the thermal conductance coming from the upper cutoff frequency decays exponentially with the inverse temperature [see Eq. (5)]. In our study, we therefore focus on the third condition, the necessary existence of transmission unity. In this case, one might expect that deviations should be present at all temperatures in any chain exhibiting an inhomogeneity that causes scattering effects. Indeed, in a variety of numerical studies on inhomogeneous systems, a reduction of the thermal conductance from its quantized value has been found, for instance, in the presence of scattering from substructures [15,16], surface roughness [17], or structural defects [18]. Such effects are also observable experimentally [14]. However, it is also observed that scattering effects of the relevant occupied long-wavelength phonons become smaller with decreasing T.

For a deeper understanding of these phenomena, it would be desirable to have analytical tools for quantum heat transport which, unfortunately, are very rare in the literature. Analytical formulas exist for a single junction [19,20] (SJ) between two homogeneous contact chains (no device) or a double junction [19,21] (DJ) consisting of a homogeneous device chain sandwiched between two homogeneous contact chains. In the theory for the DJ in Ref. [21], the characteristic Fabry-Perot multiple reflections (MR) are derived as a geometric series of reflections in the SJ system with appropriate phase factors. A further MR-approach is given in Ref. [19] based on the scattering boundary method.

We develop an analytical theory for quantum heat transport in a very general, one-dimensional contact-device-contact system consisting of an arbitrary scattering area (device) sandwiched between two homogeneous, not necessarily identical contacts (see Fig. 1). In our model, we include only nearest-neighbor interaction and neglect the influence of external potentials [22,23] as well as anharmonic effects, which is allowed for device lengths below about 20 nm at room temperature [24,25] and correspondingly longer devices at low temperatures. Using the nonequilibrium Green's function (NEGF) formalism [21,26–29], we derive an expression for the frequency-dependent heat current transmission function $\Xi(\omega)$. This compact expression allows for the analytical evaluation of

*matkaeso@physik.tu-cottbus.de
†wulf@physik.tu-cottbus.de

 ©2014 American Physical Society

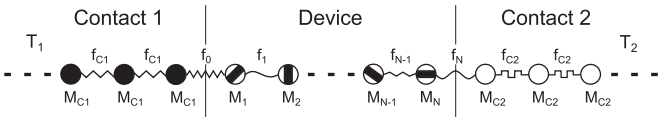

FIG. 1. Schematic representation of a one-dimensional contact-device-contact structure with a arbitrary scattering area (device) coupled to two homogeneous, not necessarily identical contacts.

the first few terms in a power series expansion of $\Xi(\omega)$ around $\omega = 0$. Applying this expansion in a Landauer-type formula [30–32], one is able to derive a systematic low-temperature expansion of the thermal conductance.

This expansion shows that quantized thermal conductance occurs for an arbitrary scattering area within second order of the temperature expansion if and only if the product of force constant and oscillator mass is identical in both contacts. We give an expression for the temperature T_ϵ above which third-order effects in the temperature have to be taken into account for a given atomic wire. Therefore this temperature determines the range on which our expansion is valid. Most interestingly, we find that quantized thermal conductance is not excluded in completely heterogeneous quasi one-dimensional systems of the considered contact-device-contact shape. Therefore thermal quantization seems to be more robust than expected from previous investigations [5,7,14].

Finally, our general formalism is illustrated and confirmed analyzing the thermal conductance of a DJ system. For the relevant frequencies below the maximum frequency in the device, we find exact agreement with Ref. [19]. As expected, a plateau in $\Lambda(T)/T$ corresponding to the quantization of the thermal conductance is found in the DJ system. In addition, our investigation show the formation of a second, lower plateau for higher temperatures. This plateau is the first phenomenon arising for temperatures beyond our low-temperature expansion. We demonstrate that it is associated with a thermal phase averaging in the scattering states. Finally, for temperatures beyond, the second plateau $\Lambda(T)/T$ decreases and the curves for different numbers of atoms merge as has been seen in numerical calculations [10,26,33].

The article is organized as follows. In Sec. II, we present the model and derive the low-temperature expansion of the ballistic thermal conductance including first interpretations and discussions. The analysis in Sec. II is based on specific properties of the phonon current transmission, which is calculated in detail in Sec. III. Our general results in Secs. II and III are applied for a DJ system in Sec. IV.

II. LOW-TEMPERATURE EXPANSION OF THE THERMAL CONDUCTANCE

We consider phononic heat transport in a one-dimensional chain of atoms in nearest-neighbor interaction with a contact-device-contact structure as depicted in Fig. 1. The parameters f_i denote the coupling strengths between the ith atom with mass M_i and the $(i+1)$th atom. In our model, the device consists of N atoms, $i = 1,\ldots,N$, with arbitrary f_i and M_i. The two contacts, $s = 1$ for $i \leqslant 0$ and $s = 2$ for $i \geqslant N+1$, are taken to be homogeneous but not necessarily identical, $f_{i\leqslant 0} = f_{C1}$, $f_{i\geqslant N+1} = f_{C2}$, $M_{i\leqslant 0} = M_{C1}$, and $M_{i\geqslant N+1} = M_{C2}$. The contacts themselves serve as thermodynamic reservoirs with the constant individual temperatures T_s. Assuming ballistic transport, the heat flux takes the typical Landauer form [26,30–32]

$$J(T_1,T_2) = \int_0^\Omega \frac{\hbar\omega}{2\pi}\Xi(\omega)[N(\omega,T_1) - N(\omega,T_2)]d\omega. \quad (1)$$

The function $N(\omega,T) = 1/[\exp(\hbar\omega/k_BT) - 1]$ is the Bose-Einstein-distribution, $\Xi(\omega)$ is the transmission function for the heat current, and $\Omega := \min\{\omega_s^{\max}, s = 1,2\}$ is the lower of the two maximum frequencies in the contacts. From Eq. (1), we find the thermal conductance

$$\begin{aligned}\Lambda(T) &= \lim_{\Delta T\to 0}\frac{J(T,T')}{\Delta T}\\ &= \int_0^\Omega \frac{\hbar\omega}{2\pi}\Xi(\omega)\frac{\partial N(\omega,T)}{\partial T}d\omega\\ &= \sum_{k=0}^\infty \frac{\Xi_{2k}}{(2k)!}\int_0^\Omega \frac{\hbar\omega^{2k+1}}{2\pi}\frac{\partial N(\omega,T)}{\partial T}d\omega \end{aligned} \quad (2)$$

with $\Delta T = T - T'$. In the last step of Eq. (2), we use a Taylor expansion of the transmission function around $\omega = 0$ and assume the interchangeability of the summation and the integration. As we will see in the next section, in a general oscillator chain $\Xi(\omega)$ is an even function so that uneven terms in the Taylor expansion around $\omega = 0$ vanish. Upon introduction of the variables $x := \hbar\omega/k_BT$ and $\beta := k_BT/\hbar\Omega$ a dimensionless expression for the thermal conductance follows as

$$\lambda(\beta) = \frac{\Lambda}{\Lambda_\infty} = \sum_{k=0}^\infty \frac{\Xi_{2k}\Omega^{2k}}{(2k)!}\left[\int_0^{1/\beta}\frac{x^{2(k+1)}e^x}{(e^x-1)^2}dx\right]\beta^{2k+1}, \quad (3)$$

where $\Lambda_\infty = k_B\Omega/2\pi$ is the thermal conductance of the homogeneous chain corresponding to the contact with the lower maximum frequency at $T\to\infty$. Carrying out the integration, the normalized thermal conductance takes the form

$$\lambda(\beta) = \sum_{k=0}^\infty \frac{2(k+1)!}{(2k)!}\zeta[2(k+1)]\Xi_{2k}\Omega^{2k}\beta^{2k+1} - \lambda_{2k}(\beta), \quad (4)$$

with Riemann's zeta function $\zeta[2(k+1)]$. Here, from the existence of the maximum phonon frequency Ω, an additional correction term arises with

$$\begin{aligned}\lambda_{2k}(\beta) &= \frac{\Xi_{2k}\Omega^{2k}}{(2k)!}\left[\int_{1/\beta}^\infty \frac{x^{2(k+1)}e^x}{(e^x-1)^2}dx\right]\beta^{2k+1}\\ &\approx \frac{\Xi_{2k}\Omega^{2k}}{(2k)!}\frac{e^{-1/\beta}}{\beta}. \end{aligned} \quad (5)$$

For the second step of (5), we include the leading-order term only which results from an expansion of the integrand for large x (small temperatures). From this leading-order term, it is evident that $\lambda_{2k}(\beta)$ can be practically always neglected for low temperatures because of the exponential decay with $1/\beta$. Then with Eq. (4) we can express the low-temperature

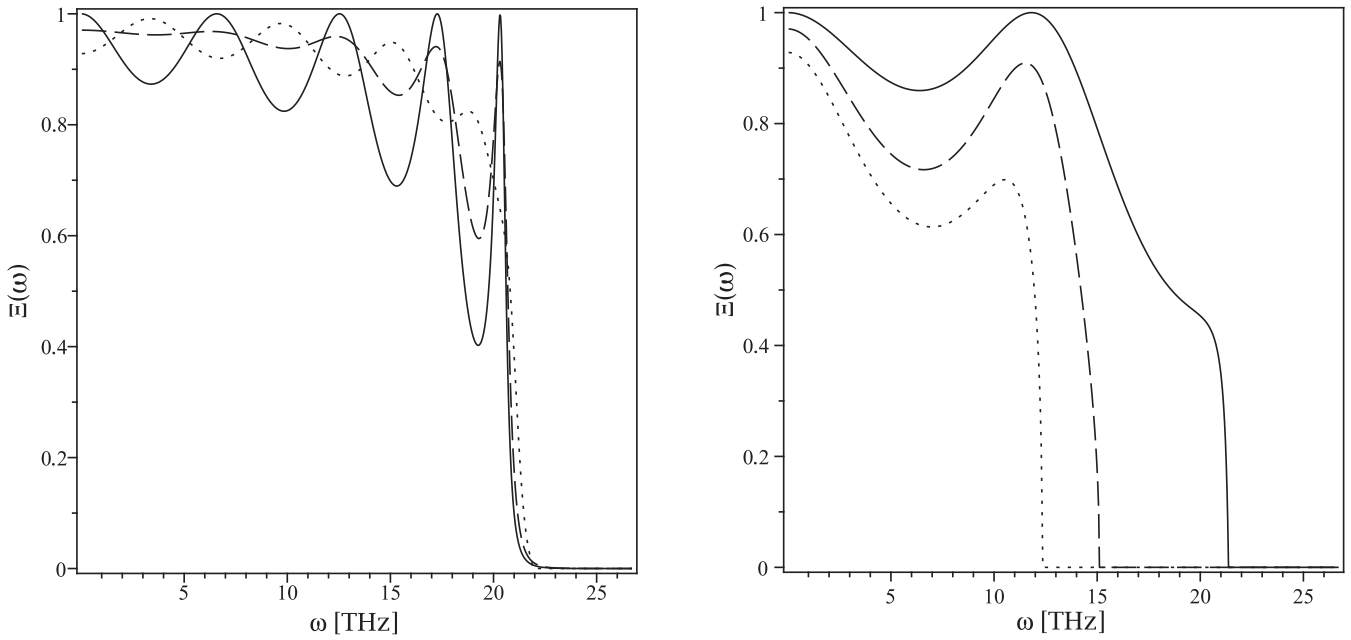

FIG. 2. Current transmission according to Eq. (17) for DJ structures with $N = 5$. (Left) Si-Ge-Si$_X$ with M_X equal to M_{Si} (solid), $2M_{\mathrm{Si}}$ (dashed), and $3M_{\mathrm{Si}}$ (dotted). (Right) Ge-Si-Ge$_X$ with M_X equal to M_{Ge} (solid), $2M_{\mathrm{Ge}}$ (dashed), and $3M_{\mathrm{Ge}}$ (dotted). Further parameters are taken from Ref. [10]: $M_{\mathrm{Si}} = 4.7 \times 10^{-26}$ kg, $f_{\mathrm{Si}} = 16.9$ N/m, $d_{\mathrm{Si}} = 5.43 \times 10^{-10}$, $M_{\mathrm{Ge}} = 1.2 \times 10^{-25}$ kg, $f_{\mathrm{Ge}} = 13.7$ N/m, and $d_{\mathrm{Ge}} = 5.66 \times 10^{-10}$ m. In addition, $f_0 = (f_{C1} + f_D)/2$, and $f_N = (f_D + f_{C2})/2$.

thermal conductance in a third-order expansion as

$$\lambda(\beta) = \frac{\pi^2}{3}\Xi_0\beta + \frac{2\pi^4}{15}\Xi_2\Omega^2\beta^3. \tag{6}$$

As shown below, this concise representation is sufficient to discuss the most important properties of the low-temperature thermal conductance of a very general one-dimensional contact-device-contact system.

The quantized thermal conductance is given by $(\pi^2/3)\beta$. Therefore it follows from the inspection of the leading-order term in Eq. (6) that the quantized thermal conductance occurs, within second order of the temperature expansion if and only if $\Xi_0 = 1$. To explore this condition, an exact expression

$$\Xi_0 = \frac{4\sqrt{y}}{[1+\sqrt{y}]^2} \tag{7}$$

will be derived in the next section which is valid for an arbitrary oscillator chain as depicted in Fig. 1. The condition $\Xi_0 = 1$ is found to hold for all chains with $y := M_{C2}f_{C2}/M_{C1}f_{C1} = 1$, independent of the scattering area, i.e., the contacts do not have to be equal only the product of mass and coupling constant does. Therefore it is not excluded to observe quantized thermal conductance in a completely heterogeneous contact-device-contact setup. For all chains not meeting this condition, the thermal conductance is reduced by a factor of $\Xi_0 < 1$ below its quantum value.

For the physical interpretation of (7), we consider the acoustic mismatch model (AMM) [34]. This low-temperature theory describes the transport of phonons across a SJ separating two different materials. Assuming complete specular scattering, the AMM-transmission function is given by $\Xi_{\mathrm{AMM}}(\omega) = 4Z_1Z_2/(Z_1+Z_2)^2$ with $Z_s = \rho_s v_s(\omega)$ as the acoustic impedance. For our one-dimensional problem, $\rho_s = M_{Cs}/d_{Cs}$ is the length mass density and $v_s(\omega) = d\omega(k_s)/dk_s = (d_s\omega_s^{\max}/2)\cos[k_s(\omega)d_s/2]$ (see Sec. III) the group velocity of the phonons. At small frequencies, we can write $v_s(\omega \to 0) = d_s\omega_s^{\max}/2$ yielding $\Xi_{\mathrm{AMM}}(\omega \to 0) = \Xi_0$ as represented in Eq. (7). From this result it follows that at low temperatures the transport problem with a arbitrary scattering area behaves like a SJ problem in which the contacts are coupled directly. Now it is possible to express our condition for quantized thermal conductance as $y = Z_2^2(\omega \to 0)/Z_1^2(\omega \to 0) = 1$. If the volumetric mass density is used, $\Xi_{\mathrm{AMM}}(\omega)$ is also valid for three-dimensional systems. Therefore we assume that under certain prerequisites the condition $y = 1$ for the quantized thermal conductance is applicable for each acoustic mode in the greater class of quasi-one-dimensional systems separately.

For increasing temperatures, it can be taken from (6) that the leading-order linear term is corrected by a cubic term $\propto T^3$, which can be, in general, smaller or larger than zero depending on the expansion coefficient Ξ_2 (see Fig. 2 as well as for example Fig. 7 of Ref. [24]). It is seen that for $\Xi_2 > 0$ ($\Xi_0 < 1$) a suitable device region improves the thermal conduction compared to the SJ system in which one connects the contacts directly (AMM). This is in analogy to the blooming coat in optics. Such an effect is not possible in classical diffusive heat transport in which thermal resistances add. If we obtain quantized thermal conductance ($\Xi_0 = 1$), then it is always $\Xi_2 < 0$ and the thermal conductance is reduced. In our case, this behavior is caused by the scattering of phonons at the device region for increasing temperatures. In other cases of heterogeneous nanosystems, a similar behavior was also found and it can be always attributed to different scattering

mechanisms like scattering on sub structures [15,16], by surface roughness [17], or structural defects [18]. Such an effect is also observable in experiment [14].

To quantify the precision of the quantization of thermal conductance, we introduce the ratio of the correction term to the leading-order term in Eq. (6) $\epsilon = (2\pi^4/15)\Xi_2\Omega^2\beta^3/(\pi^2/3)\Xi_0\beta$. Then, for a given precision requirement ϵ, an upper temperature

$$T_\epsilon = \frac{\hbar}{\pi k_B}\sqrt{\epsilon\frac{5\Xi_0}{2\,|\Xi_2|}} \tag{8}$$

results for the occurrence of the plateau associated with the quantization of the thermal conductance (see Fig. 4). The quantity T_ϵ can thus be interpreted as the width of the quantized conductance plateau.

III. CALCULATION OF PHONON CURRENT TRANSMISSION

Starting point for the evaluation of the phonon current transmission in our oscillator chain is the general expression in the NEGF formulation [26]

$$\Xi(\omega) = \mathrm{Tr}[\Gamma_1(\omega)G_D(\omega)\Gamma_2(\omega)G_D^+(\omega)]. \tag{9}$$

Here,

$$[G_D(\omega)] := [\omega^2 I - D_D - \Sigma_1(\omega) - \Sigma_2(\omega)]^{-1} \equiv [M_N(\omega)]^{-1} \tag{10}$$

is the $(N \times N)$ Green's matrix of the device with its hermitian transpose $[G_D]^+$ and the identity matrix $[I]$. The explicit form of the dynamic matrix $[D_D]$ in our oscillator chain and the form of the other relevant matrices $[\Gamma_s(\omega)]$ and $[\Sigma_s(\omega)]$ is derived in Appendix A. It results that $[M_N(\omega)]$ is a tridiagonal matrix of the form

$$[M_N(\omega)] = \begin{bmatrix} a_1(\omega) & b_1 & 0 & \cdots & 0 \\ b_1 & a_2(\omega) & \ddots & \ddots & \vdots \\ 0 & \ddots & \ddots & \ddots & 0 \\ \vdots & \ddots & \ddots & a_{N-1}(\omega) & b_{N-1} \\ 0 & \cdots & 0 & b_{N-1} & a_N(\omega) \end{bmatrix}. \tag{11}$$

Here, the individual matrix elements are defined as follows. For $2 \leqslant i \leqslant N-1$, we have $a_i(\omega) = \omega^2 - (f_{i-1} + f_i)/M_i$ and, for $1 \leqslant i \leqslant N-1$, one has $b_i = f_i/\sqrt{M_i M_{i+1}}$. Furthermore, one obtains

$$a_1(\omega) = \omega^2 - \frac{f_0 + f_1}{M_1} - \frac{f_0^2}{M_{C1}M_1}g_1(\omega) \tag{12}$$

and

$$a_N(\omega) = \omega^2 - \frac{f_{N-1} + f_N}{M_N} - \frac{f_N^2}{M_N M_{C2}}g_2(\omega). \tag{13}$$

To describe a contact-device-contact structure with the matrix (11), we have to choose $N \geqslant 2$. The functions $g_s(\omega)$ are the (1×1) surface Green's matrices (see, e.g., Refs. [26,35])

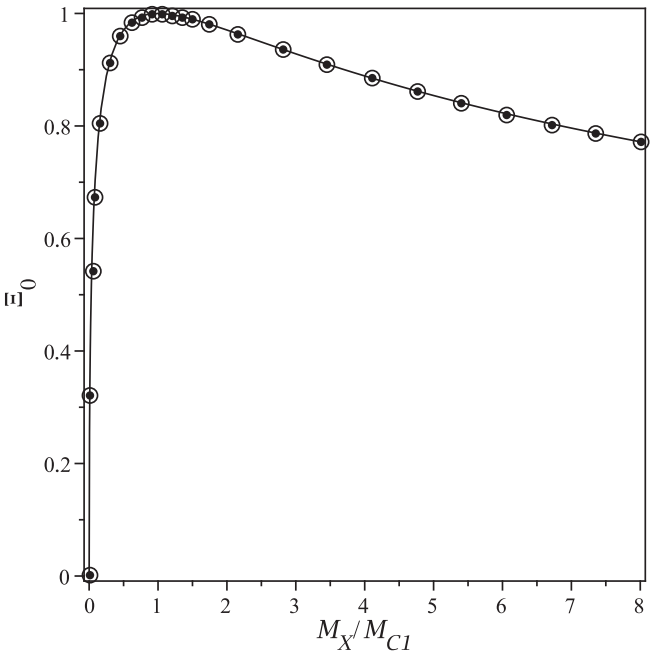

FIG. 3. Representation of $\Xi(\omega \to 0) = \Xi_0$ as a function of the ratio of the contact masses $y = M_X/M_{C1}$. Points: for a Si-Ge-Si$_X$ structure with a device region consisting of five Ge atoms and a Si contact. Circle: for a Ge-Si-Ge$_X$ structure with a device region consisting of five Si atoms and a Ge contact. The points and circles are calculated from (17) and the solid line is calculated from the universal result (7).

corresponding to the uncoupled contacts given by

$$g_1(\omega) = \left[(\omega + i0^+)^2 - \frac{f_{C1} + f_0}{M_{C1}} + \frac{f_{C1}}{M_{C1}}e^{ik_1(\omega)d_1}\right]^{-1} \tag{14}$$

and

$$g_2(\omega) = \left[(\omega + i0^+)^2 - \frac{f_N + f_{C2}}{M_{C2}} + \frac{f_{C2}}{M_{C2}}e^{ik_2(\omega)d_2}\right]^{-1}. \tag{15}$$

The expression $k_s(\omega) = (2/d_s)\arcsin(\omega/\omega_s^{\max})$ is the dispersion relation and d_s is the lattice constant in contact s. The maximum frequencies in the respective contacts are given by $\omega_s^{\max} = 2\sqrt{f_{Cs}/M_{Cs}}$. (Note, if i is not used as a subscript, it has the meaning of the imaginary unit.)

In Appendix B, we show that from Eqs. (9)–(11) the current transmission function in our oscillator chain can be written in the form

$$\Xi(\omega) = C\frac{\gamma_1(\omega)\gamma_2(\omega)}{|\det[M_N(\omega)]|^2} \quad \text{with} \quad C = \prod_{i=1}^{N-1}\frac{f_i^2}{M_i M_{i+1}}, \tag{16}$$

where $\gamma_s(\omega) = C_s[g_s(\omega) - g_s^*(\omega)]$, $C_1 = if_0^2/M_{C1}M_1$, and $C_2 = if_N^2/M_N M_{C2}$. Using Eq. (16) it is not necessary to invert the matrix $[M_N(\omega)]$ in contrast to the fundamental equation of transmission (9). It is merely necessary to calculate a determinant for which an analytical low-frequency expansion can be established as demonstrated in Appendix C. The central result of this expansion is the expression for Ξ_0 given in Eq. (7). Finally, starting from (16) we show also in Appendix B that

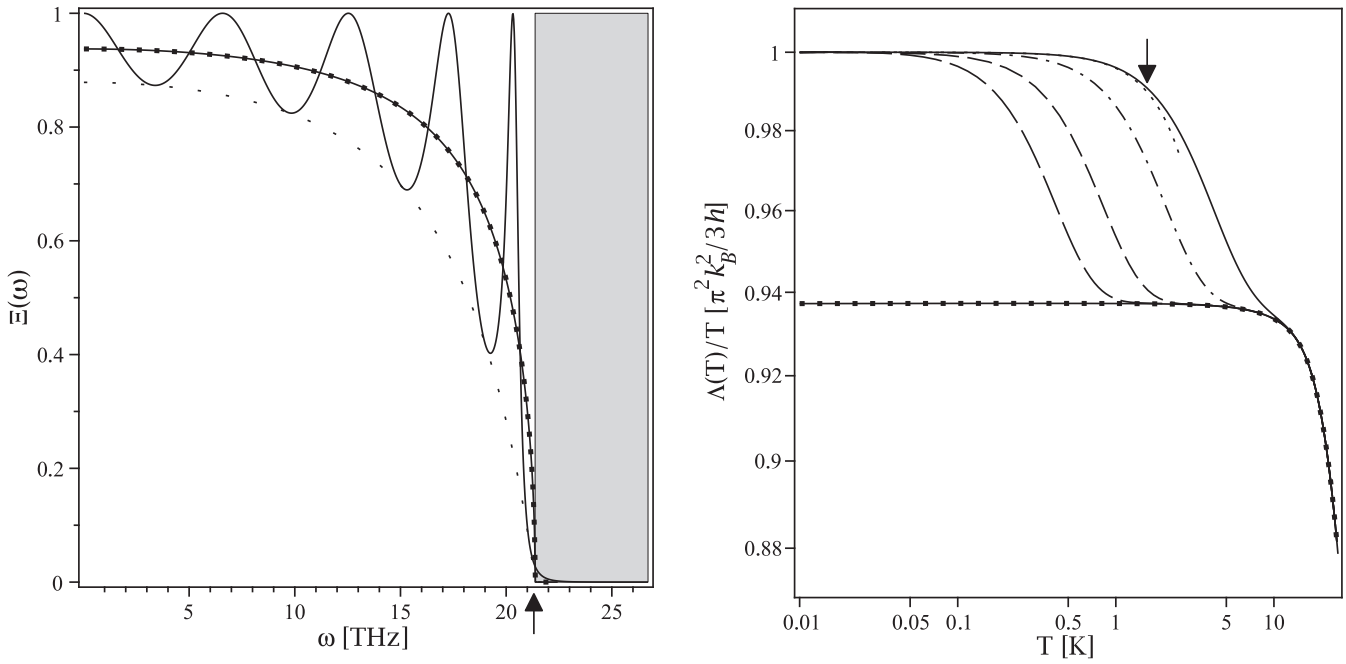

FIG. 4. (Left) Transmission for a Si-Ge-Si DJ structure with a device region consisting of five Ge atoms (solid) as well as the averaged transmission according to Eq. (19) (solid line with points). The peaks resulting from multiple reflections between the two interfaces of the DJ system. The minima of the transmission are enveloped by the square of the averaged transmission function (dotted). The arrow marked the maximum device frequency $2\tilde{\omega}_0 = 21.4$ THz. In the "forbidden" gray region above $2\tilde{\omega}_0$, we observe phonon tunneling as the small tail. (Right) Thermal conductance $\Lambda(T)$ divided by T for a Si-Ge-Si DJ structure with a device region consisting of 5 (solid), 10 (dashed dotted), 25 (dashed), and 50 (long dashed) Ge–atoms. The upper plateau corresponds to the quantum of the thermal conduction. We see also the forming of a second plateau for increasing the number of atoms in the device with the value (20). The dotted line represents the expansion corresponding to Eq. (6) for a device consisting of five atoms. The arrow indicates the plateau width $T_\epsilon = 1.6$ K according to a deviation of the thermal conductance from the quantum value of about 1% ($\epsilon = 0.01$). All curves for different N merge with a asymptote (solid line with points), which is given by $\Lambda_{\rm av}(T)/T$.

$\Xi(\omega)$ is an even function and therefore the assumed Taylor expansion of $\Xi(\omega)$ in Eq. (2) has indeed no uneven terms.

IV. APPLICATION TO THE DJ ATOMIC WIRE

To illustrate our analytical results, we consider a DJ chain of two homogeneous contacts and a homogeneous device region between them, $M_i = M_D$ and $f_i = f_D$ for $1 \leqslant i \leqslant N$. Because of the homogeneous device area, one has in Eq. (11) $a_{2\leqslant i\leqslant N-1}(\omega) := \omega^2 - 2\tilde{\omega}_0^2$ and $b_{1\leqslant i\leqslant N-1} := \tilde{\omega}_0^2$ with $\tilde{\omega}_0^2 := f_D/M_D$ where in Eqs. (14) and (15) we choose $f_1 = f_{N-1} := f_D$ as well as $M_1 = M_N := M_D$.

Starting from this setup, we evaluate (16) in Appendix D to obtain for $N \geqslant 3$

$$\Xi(\omega) = \frac{C\gamma_1(\omega)\gamma_2(\omega)}{\left|a_1 a_N n_{N-2} - \tilde{\omega}_0^4(a_1 + a_N)n_{N-3} + \tilde{\omega}_0^8 n_{N-4}\right|^2} \quad (17)$$

with $n_{-1} := 0$, $n_0 := 1$, and

$$n_L(\omega) = \prod_{n=1}^{L}\left\{\omega^2 - 4\tilde{\omega}_0^2 \sin^2\left[\frac{n\pi}{2(L+1)}\right]\right\}. \quad (18)$$

Here, we have suppressed the explicit frequency dependence in various variables.

This formula is applied to a Si-Ge-Si_X structure with one Si contact and a device consisting of five Ge atoms. In the other contact, Si_X symbolizes a fictitious type of isotopes with the same spring constant like in Si but a different mass M_X. The evaluation of (17) leads to typical transmission curves depicted in Fig. 2. For comparison, the transmission for a Ge-Si-Ge_X structure is represented in Fig. 2 as well. In both cases, $\Xi(\omega \to 0) = \Xi_0$ is not always equal to one. Then, from the first term $(\pi^2/3)\Xi_0\beta$ in Eq. (6) a deviation from the quantized thermal conductance follows. According to Eq. (7), this deviation only depends on the structure of the contacts, namely, on the parameter $y = M_{C1}f_{C1}/M_{C2}f_{C2}$. To demonstrate this result, we have plotted in Fig. 3 for the considered chains the value of $\Xi(\omega \to 0) = \Xi_0$ as deduced from (17) and Ξ_0 as deduced from Eq. (7). Complete agreement is found for both chain types and all considered ratios M_X/M_{C1}. As expected, only for $M_X = M_{C1}$ and thus for $y = 1$, we obtain $\Xi_0 = 1$ yielding universal quantized thermal conductance, independent of the scattering area.

In Fig. 4, we analyze more precisely the NEGF-transmission (17) for the Si-Ge-Si chain in Fig. 2 ($M_X = M_{\rm Si}$) and find exact agreement with Ref. [19] in the "allowed" region of frequencies below the maximum device frequency $2\tilde{\omega}_0 = 21.4$ THz, which is marked by an arrow. The effect of phonon tunneling, which is possible in general [36] and visible as the small tail in the "forbidden" gray region ($\omega > 2\tilde{\omega}_0$) was not discussed in Ref. [19]. However, for long enough devices the tunneling effect vanishes. Then, one can use Eq. (16) from

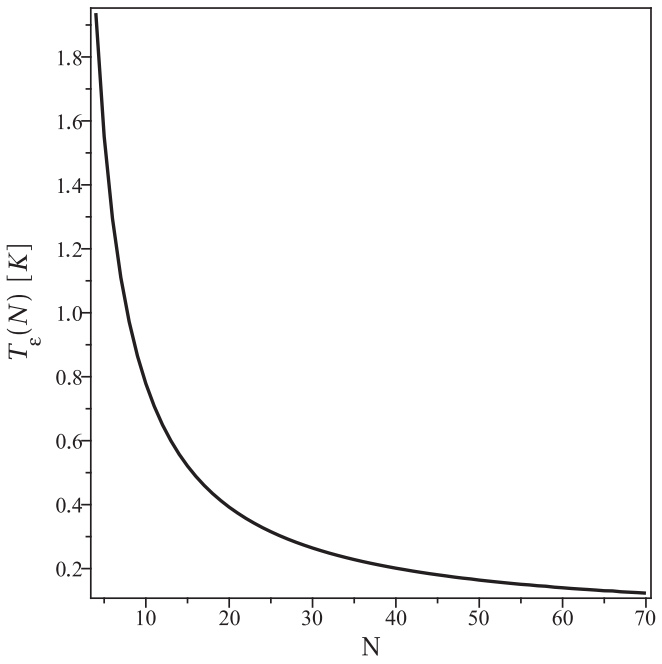

FIG. 5. The plateau width T_ϵ of the Si-Ge-Si DJ structure in Fig. 4 as a function of the device length N. We choose $\epsilon = 0.01$ corresponding to a maximum deviation of the thermal conductance from its quantized value by 1%.

Ref. [19] to obtain straightforwardly (see Ref. [21], p. 199) a simple phase-averaged expression,

$$\Xi_{\rm av}(\omega) = \frac{\Xi_{\rm SG}^2(\omega)}{1-[1-\Xi_{\rm SG}(\omega)]^2}, \tag{19}$$

for the transmission, which is depicted as the solid line with points in the left picture of Fig. 4. In Eq. (19), $\Xi_{\rm SG}(\omega)$ is the transmission of a SJ system consisting of Si and Ge, which can be easily calculated, for example, from Eq. (17) by considering a Si-Ge-Ge structure for $N = 3$.

Finally, we calculate the overall thermal conductance from Eqs. (2) and (17) for a series of Si-Ge-Si DJ chains with different device lengths (5, 10, 25, 50 atoms) plotted in the right picture of Fig. 4 in the typical representation $\Lambda(T)/T$. Since $y = 1$ in the systems, one finds for small temperatures $T < T_\epsilon$ an upper plateau at $\pi^2 k_B^2/3h$, which corresponds to the quantized thermal conductance. The width of this plateau T_ϵ is given by Eq. (8) and for the device of five atoms marked by an arrow with $\epsilon = 0.01$ according to a deviation of 1%. For higher temperatures, the third-order term of the low-temperature expansion in Eq. (6) is gaining influence and $\Lambda(T)/T$ decreases below its plateau value, which depends sensitively on N. In Fig. 5, we have plotted the plateau width T_ϵ as a function of the device length N. At yet higher temperatures, exceeding the range of our third-order expansion, the curves for different N merge with a single asymptotic curve. This asymptote results from the phase-averaged thermal conductance $\Lambda_{\rm av}(T)$ calculated from the averaged transmission in Eq. (19). It shows a lower plateau for $\Lambda_{\rm av}(T)/T$ at the value of

$$\frac{\Xi_{0,\rm SG}^2}{1-(1-\Xi_{0,\rm SG})^2}\frac{\pi^2 k_B^2}{3h}, \tag{20}$$

which is obtained from (2) and (19) for $\Xi_{\rm SG}(\omega \to 0) = \Xi_{0,\rm SG}$ with $\Xi_{0,\rm SG}$ given in Eq. (7).

For temperatures beyond the lower plateau, the trace $\Lambda(T)/T$ drops again. The described convergence of the thermal conductance against the phase-averaged value for increasing temperatures offers a natural explanation for the independence of $\Lambda(T)$ of the number of atoms in the device, found in numerical calculations [10,26,33].

V. CONCLUSION

We derived the low-temperature expansion of the ballistic thermal conductance in a very general, one-dimensional contact-device-contact system. Quantized thermal conductance is found within second order of the temperature expansion whose leading-order term yields the condition that the quantized value occurs if and only if the product of force constant and oscillator mass is identical in both contacts. This result is independent of the scattering area and explained invoking the AMM valid for a SJ system. From this discussion, it seems that the concept of the quantized thermal conductance is more robust than expected. However, above a certain temperature T_ϵ a finite-temperature correction must be taken into account leading to a deviation from the ideal value of quantization which follows a T^3-behavior. In our case it is caused by the scattering of the phonons at the device area. Further investigations of the DJ atomic wire illustrated and confirmed our general results. In this context, we found two plateaus in the representation of $\Lambda(T)/T$. The first one corresponds to the expected quantized thermal conductance present at low temperatures, while the second one at slightly higher temperatures is in a close relation to a more classical picture of transport. This can be understood by the expression (19), which is also interpretable as the transmission of a classical particle (see Ref. [21], pp. 63) in which we neglect any phase information. We see for high enough temperatures that we can not differentiate between the quantum and the classical particle picture by a measurement of the thermal conductance whereas for low temperatures there is significant difference. In the transition area between both plateaus, we obtained a clear dependence of the thermal conductance on the device length. At even higher temperatures, this dependence vanishes as expected for our ballistic transport regime.

ACKNOWLEDGMENT

This work was supported by the "Junior Research Group: Hybride Systeme" of the Brandenburg University of Technology Cottbus, Germany.

APPENDIX A: APPLICATION OF THE NEGF-FORMALISM TO A ONE-DIMENSIONAL CONTACT-DEVICE-CONTACT SETUP

In this Appendix, the relevant matrices entering the Green's matrix in Eq. (10) are constructed recapitulating the general

formalism described in Refs. [26,37]. We begin with the dynamic matrix

$$[D]_{i,j} = D_{i,j} = \frac{1}{\sqrt{M_i M_j}} \left(\frac{\partial^2 V}{\partial u_i \partial u_j} \right)_{\underline{R}^0}. \tag{A1}$$

Here, M_i is the mass of the ith atom and u_i its displacement from its equilibrium position. The vector $\underline{R}^0$ consists of the equilibrium coordinates of all atoms and the vector $\underline{u}$ of coordinates of their displacements. For a one-dimensional structure and nearest-neighbor interaction, the underlying crystal potential takes the form

$$V(\underline{u}) = \frac{1}{2} \sum_{i=-\infty}^{\infty} f_i (u_{i+1} - u_i)^2 \tag{A2}$$

leading to

$$D_{i,j} = \begin{cases} -f_{i-1}/\sqrt{M_i M_{i-1}} & \text{for } j = i-1, \\ (f_{i-1} + f_i)/\sqrt{M_i M_i} & \text{for } j = i, \\ -f_i/\sqrt{M_i M_{i+1}} & \text{for } j = i+1, \\ 0 & \text{else.} \end{cases} \tag{A3}$$

This tridiagonal matrix can be divided in a standard way into submatrix blocks of the form

$$[D] = \begin{bmatrix} D_1 & \tau_1^+ & 0 \\ \tau_1 & D_D & \tau_2 \\ 0 & \tau_2^+ & D_2 \end{bmatrix}. \tag{A4}$$

Here, the matrix $[D_D]_{i,j}$ ($i,j \in [1,N]$ see Fig. 1) describes the dynamics of the device, while the semi-infinite matrices $[D_s]$ represent the dynamics of the contact regions $s = 1,2$. These three system components are coupled via the $(N \times \infty)$-dimensional coupling matrices

$$[\tau_1]_{i,j} = t_1 \delta_{i,1} \delta_{j,0} \quad \text{for} \quad 1 \leqslant i \leqslant N,\ j \leqslant 0, \tag{A5}$$

and

$$[\tau_2]_{i,j} = t_2 \delta_{i,N} \delta_{j,N+1} \quad \text{for} \quad 1 \leqslant i \leqslant N,\ j \geqslant N+1. \tag{A6}$$

The matrix elements t_s are given by $t_1 = f_0/\sqrt{M_{C1} M_1}$ and $t_2 = f_N/\sqrt{M_N M_{C2}}$. The contact self-energy matrices take the general form

$$[\Sigma_s(\omega)] = [\tau_s][g_s(\omega)][\tau_s]^+. \tag{A7}$$

In this matrix product, $[g_s(\omega)] = [(\omega + i0^+)^2 I - D_s]^{-1}$ denotes the Green's matrices of the uncoupled contacts. In our case, the $[g_s(\omega)]$ are given by Eqs. (14) and (15). From Eq. (A7), we calculate the self-energy matrices to find

$$[\Sigma_s(\omega)]_{i,j} = (\delta_{1,s}\delta_{i,1}\delta_{j,1} + \delta_{2,s}\delta_{i,N}\delta_{j,N}) t_s^2 g_s(\omega). \tag{A8}$$

Applying the general definition

$$[\Gamma_s(\omega)] = i[\Sigma_s(\omega) - \Sigma_s^+(\omega)], \tag{A9}$$

we obtain for the oscillator chain

$$[\Gamma_s(\omega)]_{i,j} = (\delta_{1,s}\delta_{i,1}\delta_{j,1} + \delta_{2,s}\delta_{i,N}\delta_{j,N}) \gamma_s(\omega). \tag{A10}$$

Here, the functions $\gamma_s(\omega)$ are introduced in connection with Eq. (16).

APPENDIX B: CURRENT TRANSMISSION

For a general matrix $[G_D(\omega)]_{ij} = G_{ij}(\omega)$ insertion of Eq. (A10) in Eq. (9) yields

$$\Xi(\omega) = \gamma_1(\omega)\gamma_2(\omega)|G_{1N}(\omega)|^2. \tag{B1}$$

At this point, it becomes evident that it is not necessary to invert the entire $(N \times N)$ matrix $[M_N(\omega)]$ in Eq. (10) to calculate the transmission, only the element $G_{1N}(\omega)$ is required. It can already be calculated from the determinant formula for the inversion of matrices,

$$G_{ij} = \frac{1}{\det[M_N(\omega)]} \mu_{ij} \quad \text{with} \quad \mu_{ij} = (-1)^{i+j} m_{ij}. \tag{B2}$$

In this equation, μ_{ij} is the cofactor which results when the ith row and the jth column is removed from $[M_N(\omega)]^T = [M_N(\omega)]$ to form a submatrix with determinant m_{ij}. In our case, the relevant cofactor μ_{1N} can be easily calculated because deleting the first row and the last column in the matrix $[M_N(\omega)]$ leads to an upper triangular matrix with the main diagonal elements given by b_i. We thus obtain for the determinant:

$$\mu_{1N} = (-1)^{1+N} \prod_{i=1}^{N-1} b_i = (-1)^{N-1} \prod_{i=1}^{N-1} \frac{f_i}{\sqrt{M_i M_{i+1}}}. \tag{B3}$$

Substituting this result into Eq. (B2) and subsequently into Eq. (B1), we find the compact representation of the current transmission (16).

Now, we can show that $\Xi(\omega)$ is an even function. From Eq. (16), it follows

$$\begin{aligned} \gamma_s(-\omega) &= iC_s[g_s(-\omega) - g_s^*(-\omega)] \\ &= iC_s[g_s^*(\omega) - g_s(\omega)] = -\gamma_s(\omega), \end{aligned} \tag{B4}$$

which means that $\gamma_s(\omega)$ is an uneven function and therefore $\gamma_1(\omega)\gamma_2(\omega)$ is even. Furthermore, with the definitions for the matrix elements from Sec. III it is easy to show that $m_N(-\omega) := \det[M_N(-\omega)] = \det[M_N^*(\omega)] = m_N^*(\omega)$. Then

$$\begin{aligned} |m_N(-\omega)|^2 &= m_N(-\omega) m_N^*(-\omega) \\ &= m_N^*(\omega) m_N(\omega) = |m_N(\omega)|^2, \end{aligned} \tag{B5}$$

and finally $\Xi(\omega)$ is an even function.

APPENDIX C: CURRENT TRANSMISSION AROUND $\omega = 0$

To find the limit $\Xi(\omega \to 0) = \Xi_0$, we consider Eq. (16) and expand separately the occurring functions up to first order around $\omega = 0$. For the functions $\gamma_{1/2}(\omega)$, we get directly

$$\gamma_1(\omega) \approx \omega_1^{\max} \frac{M_{C1}}{M_1} \omega \quad \text{and} \quad \gamma_2(\omega) \approx \omega_2^{\max} \frac{M_{C2}}{M_N} \omega, \tag{C1}$$

and thus

$$\gamma_1(\omega)\gamma_2(\omega) \approx \omega_1^{\max}\omega_2^{\max} \frac{M_{C1}}{M_1} \frac{M_{C2}}{M_N} \omega^2. \tag{C2}$$

The expansion of $\det[M_N(\omega)] = m_N(\omega)$ takes slightly more effort. First of all, we expand $m_N(\omega)$ along the elements of the last row and gain the following recursive representation for the determinant:

$$m_N(\omega) = a_N(\omega) m_{N-1}(\omega) - b_{N-1}^2 m_{N-2}(\omega) \tag{C3}$$

with $m_{-1}(\omega) = 0$ and $m_0(\omega) = 1$. Here, is $m_{N-1}(\omega)$ the subdeterminant that remains after deletion of the last row and the last column in the matrix $[M_N(\omega)]$. The index $N-1$ shows that the original dimension of $[M_N(\omega)]$ is reduced by one. Analogously, we obtain $m_{N-2}(\omega)$ by removing again the last row and column of the matrix, which is underlying $m_{N-1}(\omega)$. Finally, we expand the determinants $m_{N-1}(\omega)$ and $m_{N-2}(\omega)$ along the first row. Then we can write in a recursive form,

$$m_{N-1}(\omega) = a_1(\omega) n_{N-2}(\omega) - b_1^2 n_{N-3}(\omega), \tag{C4}$$

$$m_{N-2}(\omega) = a_1(\omega) \bar{n}_{N-3}(\omega) - b_1^2 \bar{n}_{N-4}(\omega). \tag{C5}$$

The determinants $n_L(\omega)$ and $\bar{n}_L(\omega)$ no longer contain the special corner elements $a_1(\omega)$ and $a_N(\omega)$, what we will need later. Now, for the expansion of $m_N(\omega)$ around $\omega = 0$, we have first to determine $m_N(0)$. Therefore we set in Eq. (11) $\omega = 0$ and use the recursive representation in Eq. (C3) for the determinant $m_{N-q}(0)$ in which we have deleted the last q rows and columns. For $N - q = 1,2,3$, it follows

$$m_1(0) = a_1(0) m_0(0) - b_0^2 m_{-1}(0) = -\frac{f_1}{M_1},$$

$$m_2(0) = a_2(0) m_1(0) - b_1^2 m_0(0) = \frac{f_1 f_2}{M_1 M_2},$$

$$m_3(0) = a_3(0) m_2(0) - b_2^2 m_1(0) = -\frac{f_1 f_2 f_3}{M_1 M_2 M_3}.$$

It is natural to surmise that $m_j(0)$ for $j < N$ has the general form

$$m_j(0) = (-1)^j \prod_{i=1}^{j} \frac{f_i}{M_i}. \tag{C6}$$

We want to prove this assertion by mathematical induction. Assume, this assertion is true for j, then we get for $j+1$,

$$\begin{aligned} m_{j+1}(0) &= a_{j+1}(0) m_j(0) - b_j^2 m_{j-1}(0) \\ &= -\frac{f_j + f_{j+1}}{M_{j+1}} (-1)^j \prod_{i=1}^{j} \frac{f_i}{M_i} - \frac{(-1)^{j-1} f_j^2}{M_j M_{j+1}} \prod_{i=1}^{j-1} \frac{f_i}{M_i} \\ &= (-1)^j \left(-\frac{f_j}{M_{j+1}} \prod_{i=1}^{j} \frac{f_i}{M_i} - \prod_{i=1}^{j+1} \frac{f_i}{M_i} + \frac{f_j}{M_{j+1}} \prod_{i=1}^{j} \frac{f_i}{M_i} \right) \\ &= (-1)^{j+1} \prod_{i=1}^{j+1} \frac{f_i}{M_i}. \end{aligned}$$

It follows that (C6) is true for each $j < N$ with N from the natural numbers. Now, we can calculate $m_N(0)$, it is

$$\begin{aligned} m_N(0) &= a_N(0) m_{N-1}(0) - b_{N-1}^2 m_{N-2}(0) \\ &= -\frac{f_{N-1}}{M_N} (-1)^{N-1} \prod_{i=1}^{N-1} \frac{f_i}{M_i} - \frac{(-1)^{N-2} f_{N-1}^2}{M_{N-1} M_N} \prod_{i=1}^{N-2} \frac{f_i}{M_i} \\ &= (-1)^N \left(\frac{f_{N-1}}{M_N} \prod_{i=1}^{N-1} \frac{f_i}{M_i} - \frac{f_{N-1}}{M_N} \prod_{i=1}^{N-1} \frac{f_i}{M_i} \right) = 0. \end{aligned}$$

This means that the zeroth order of our expansion vanishes. For the next order, we derive the first equation in Eq. (C3) by ω and get for $\omega = 0$,

$$\frac{dm_N}{d\omega} = m_{N-1} \frac{da_N}{d\omega} + a_N \frac{dm_{N-1}}{d\omega} - b_{N-1}^2 \frac{dm_{N-2}}{d\omega}, \tag{C7}$$

where we have suppressed the argument $\omega = 0$. In this equation, we have to evaluate the expressions $dm_{N-1}(0)/d\omega$ and $dm_{N-2}(0)/d\omega$. For that, we use (C4) and (C5), which follows

$$\frac{dm_{N-1}}{d\omega} = n_{N-2} \frac{da_1}{d\omega} + a_1 \frac{dn_{N-2}}{d\omega} - b_1^2 \frac{dn_{N-3}}{d\omega}, \tag{C8}$$

$$\frac{dm_{N-2}}{d\omega} = \bar{n}_{N-3} \frac{da_1}{d\omega} + a_1 \frac{d\bar{n}_{N-3}}{d\omega} - b_1^2 \frac{d\bar{n}_{N-4}}{d\omega}. \tag{C9}$$

The determinants $n_L(\omega)$ and $\bar{n}_L(\omega)$ are polynomials of degree $2L$, whose derivative vanishes at $\omega = 0$. Thereby, Eq. (C7) takes the form

$$\frac{dm_N}{d\omega} = m_{N-1} \frac{da_N}{d\omega} + \left(a_N n_{N-2} - b_{N-1}^2 \bar{n}_{N-3} \right) \frac{da_1}{d\omega}. \tag{C10}$$

If we use our definitions for $n_L(\omega)$ and $\bar{n}_L(\omega)$, it is easy to show that the expression in brackets is one of the possible expansions of the determinant $\bar{m}_{N-1}(\omega)$. Here, $\bar{m}_{N-1}(\omega)$ is the subdeterminant, which we get when we delete the first row and column in the matrix $[M_N(\omega)]$. So, we can represent the derivative $dm_N(0)/d\omega$ by

$$\frac{dm_N(0)}{d\omega} = \bar{m}_{N-1}(0) \frac{da_1(0)}{d\omega} + m_{N-1}(0) \frac{da_N(0)}{d\omega}. \tag{C11}$$

Analogous to Eq. (C6), we can calculate $\bar{m}_j(\omega)$ and proof the result by mathematical induction. This leads to

$$\bar{m}_j(0) = (-1)^j \prod_{i=N-j+1}^{N} \frac{f_{i-1}}{M_i} \quad \text{with} \quad j \leqslant N-1. \tag{C12}$$

From (C6) and (C12), we find for $\bar{m}_{N-1}(0)$ and $m_{N-1}(0)$ the following correlation:

$$M_1 m_{N-1}(0) = M_N \bar{m}_{N-1}(0). \tag{C13}$$

Finally, we have to calculate the derivatives of the elements $a_1(\omega)$ and $a_N(\omega)$ at the point $\omega = 0$, it is

$$\frac{da_1(0)}{d\omega} = i \frac{M_{C1}}{2M_1} \omega_1^{\max} \quad \text{and} \quad \frac{da_N(0)}{d\omega} = i \frac{M_{C2}}{2M_N} \omega_2^{\max}, \tag{C14}$$

where we used the dispersion relations $k_s(\omega) = (2/d_s) \arcsin(\omega/\omega_s^{\max})$ defined in Sec. III. With (C13) and (C14), we can write for Eq. (C11):

$$\frac{dm_N(0)}{d\omega} = i \frac{m_{N-1}(0)}{2M_N} \left(M_{C1} \omega_1^{\max} + M_{C2} \omega_2^{\max} \right). \tag{C15}$$

Now, we have all details for the first-order expansion of $m_N(\omega)$ around $\omega = 0$. Especially for $|m_N(\omega)|^2$, we find then the following representation:

$$|m_N(\omega)|^2 = \frac{m_{N-1}(0)^2}{4M_N^2} \left(M_{C1} \omega_1^{\max} + M_{C2} \omega_2^{\max} \right)^2 \omega^2. \tag{C16}$$

The last step of our derivation is to insert (C2) and (C16) as well as

$$C = \prod_{i=1}^{N-1} \frac{f_i^2}{M_i M_{i+1}} = \frac{M_1}{M_N} \prod_{i=1}^{N-1} \frac{f_i^2}{M_i^2} = \frac{M_1}{M_N} m_{N-1}(0)^2 \tag{C17}$$

in Eq. (16) for $\Xi(\omega \to 0)$ resulting in

$$\Xi_0 = \frac{4M_{C1}\omega_1^{\max} M_{C2}\omega_2^{\max}}{\left(M_{C1}\omega_1^{\max} + M_{C2}\omega_2^{\max}\right)^2} = \frac{4\sqrt{M_{C1}f_{C1}}\sqrt{M_{C2}f_{C2}}}{(\sqrt{M_{C1}f_{C1}} + \sqrt{M_{C2}f_{C2}})^2}. \quad \text{(C18)}$$

With the definition $y := M_{C2}f_{C2}/M_{C1}f_{C1}$, we get finally the universal representation (7).

APPENDIX D: CURRENT TRANSMISSION FOR THE DJ ATOMIC WIRE

To derive Eq. (17), we use (C3) in which we substitute $m_{N-1}(\omega)$ and $m_{N-2}(\omega)$ by (C4) as well as (C5). In our special chain, $b_1 = b_{N-1} = \tilde{\omega}_0^2$ and $n_L(\omega) = \bar{n}_L(\omega)$ leading to

$$m_N(\omega) = a_1 a_N n_{N-2} - \tilde{\omega}_0^4[a_1 + a_N]n_{N-3} + \tilde{\omega}_0^8 n_{N-4}. \quad \text{(D1)}$$

We have suppressed the frequency dependence of $a_1(\omega)$, $a_N(\omega)$, and $n_L(\omega)$. The $n_L(\omega)$ are determinants of symmetric tridiagonal matrices with the dimensions $L = N-2$, $N-3, N-4$, which have on the main diagonal only the elements $\omega^2 - 2\tilde{\omega}_0^2$ and on the secondary diagonals only the elements $\tilde{\omega}_0^2$. In this case, the $n_L(\omega)$ corresponding to analytically solvable Toeplitz eigenvalue problems [38] with the eigenvalues

$$\omega_{L,n}^2 = 2\tilde{\omega}_0^2\left[1 - \cos\left(\frac{n\pi}{L+1}\right)\right] \text{ with } n = 1, \ldots, L. \quad \text{(D2)}$$

For the resulting diagonal matrices, the determinants $n_L(\omega)$ can be calculated easily,

$$n_L(\omega) = \prod_{n=1}^{L}\left(\omega^2 - \omega_{L,n}^2\right), \quad \text{(D3)}$$

which yields (18). Finally, from (16) and (D1), the analytical expression for $\Xi(\omega)$ in Eq. (17) follows.

[1] C. W. Chang, D. Okawa, A. Majumdar, and A. Zettl, Science **314**, 1121 (2006).
[2] B. Li, L. Wang, and G. Casati, Appl. Phys. Lett. **88**, 143501 (2006).
[3] L. Wang and B. Li, Phys. Rev. Lett. **99**, 177208 (2007).
[4] L. Wang and B. Li, Phys. Rev. Lett. **101**, 267203 (2008).
[5] A. Greiner, L. Reggiani, T. Kuhn, and L. Varani, Phys. Rev. Lett. **78**, 1114 (1997).
[6] R. Venkatesh, J. Amrit, Y. Chalopin, and S. Volz, Phys. Rev. B **83**, 115425 (2011).
[7] L. G. C. Rego and G. Kirczenow, Phys. Rev. Lett. **81**, 232 (1998).
[8] A. Buldum, S. Ciraci, and C. Y. Fong, J. Phys.: Condens. Matter. **12**, 3349 (2000).
[9] J. Zimmermann, P. Pavone, and G. Cuniberti, Phys. Rev. B **78**, 045410 (2008).
[10] P. E. Hopkins, P. M. Norris, M. S. Tsegaye, and A. W. Ghosh, J. Appl. Phys. **106**, 063503 (2009).
[11] L. G. C. Rego and G. Kirczenow, Phys. Rev. B **59**, 13080 (1999).
[12] I. V. Krive and E. R. Mucciolo, Phys. Rev. B **60**, 1429 (1999).
[13] L. G. C. Rego, Phys. Status Solidi A **187**, 239 (2001).
[14] K. Schwab, E. A. Henriksen, J. M. Worlock, and M. L. Roukes, Nature (London) **404**, 974 (2000).
[15] P. Yang, Q. F. Sun, H. Guo, and B. Hu, Phys. Rev. B **75**, 235319 (2007).
[16] F. Xie, K.-Q. Chen, Y. G. Wang, and Y. Zhang, J. Appl. Phys. **103**, 084501 (2008).
[17] D. H. Santamore and M. C. Cross, Phys. Rev. Lett. **87**, 115502 (2001).
[18] K.-Q. Chen, W.-X. Li, W. Duan, Z. Shuai, and B.-L. Gu, Phys. Rev. B **72**, 045422 (2005).
[19] L. Zhang, P. Keblinski, J.-S. Wang, and B. Li, Phys. Rev. B **83**, 064303 (2011).
[20] H. Li, B. K. Agarwalla, and J.-S. Wang, Phys. Rev. E **86**, 011141 (2012).
[21] S. Datta, *Electronic Transport in Mesoscopic Systems* (Cambridge University Press, New York, 1995).
[22] P. Tong, B. Li, and B. Hu, Phys. Rev. B **59**, 8639 (1999).
[23] S. Ma, H. Xu, H. Deng, and B. Yang, Phys. Lett. A **375**, 1831 (2011).
[24] D. Segal, A. Nitzana, and P. Hänggi, J. Chem. Phys. **119**, 6840 (2003).
[25] N. Mingo and L. Yang, Phys. Rev. B **68**, 245406 (2003).
[26] W. Zhang, N. Mingo, and T. Fisher, Numer. Heat Transfer, Part B **51**, 333 (2007).
[27] W. Zhang, N. Mingo, and T. Fisher, J. Heat Transfer **129**, 483 (2007).
[28] S. Datta, Superlattices Microstruct. **28**, 253 (2000).
[29] S. Datta, *Quantum Transport: Atom to Transistor* (Cambridge University Press, New York, 2005).
[30] R. Landauer, Philos. Mag. **21**, 863 (1970).
[31] D. C. Langreth and E. Abrahams, Phys. Rev. B **24**, 2978 (1981).
[32] M. P. Blencowe, Phys. Rev. B **59**, 4992 (1999).
[33] A. Ozpineci and S. Ciraci, Phys. Rev. B **63**, 125415 (2001).
[34] W. A. Little, Can. J. Phys. **37**, 334 (1959).
[35] J.-S. Wang, J. Wang, and J. T. Lü, Eur. Phys. J. B **62**, 381 (2008).
[36] It is possible for systems with a maximum device frequency smaller than the both maximum contact frequencies, otherwise phonon tunneling is basically not possible (see Fig. 2).
[37] G. Czycholl, *Theoretische Festkörperphysik* (Springer, Berlin, Heidelberg, 2008), pp. 39–45.
[38] M. J. C. Gover, Linear Algebra Appl. **197/198**, 63 (1994).